

## Design Improvements and R&D Achievements for VV and In-vessel Components Towards ITER Construction

K. Ioki <sup>1)</sup>, P. Barabaschi <sup>1)</sup>, V. Barabash <sup>1)</sup>, S. Chiochio <sup>1)</sup>, W. Daenner <sup>2)</sup>, F. Elio <sup>1)</sup>, M. Enoeda <sup>3)</sup>, A. Gervash <sup>4)</sup>, C. Ibbott <sup>1)</sup>, L. Jones <sup>2)</sup>, V. Krylov <sup>4)</sup>, T. Kuroda <sup>3)</sup>, P. Lorenzetto <sup>2)</sup>, E. Martin <sup>1)</sup>, I. Mazul <sup>4)</sup>, M. Merola <sup>2)</sup>, M. Nakahira <sup>3)</sup>, V. Rozov <sup>1)</sup>, Yu. Strebkov <sup>4)</sup>, S. Suzuki <sup>3)</sup>, V. Tanchuk <sup>4)</sup>, R. Tivey <sup>1)</sup>, Yu. Utin <sup>1)</sup>, M. Yamada <sup>1)</sup>

<sup>1)</sup> ITER International Team, Boltzmannstrasse 2, 85748 Garching, Germany

<sup>2)</sup> EFDA-CSU, Boltzmannstrasse 2, 85748 Garching, Germany

<sup>3)</sup> JAERI, Naka Establishment, Naka-machi, Naka-gun, Ibaraki-ken, Japan

<sup>4)</sup> NTC Sintez, Efremov Inst., 189631 Metallostroy, St. Petersburg, Russia

e-mail contact of main author: iokik@itereu.de

**Abstract.** During the preparation of the procurement specifications for long lead-time items, several detailed vacuum vessel (VV) design improvements are being pursued, such as elimination of the inboard triangular support, adding a separate interspace between inner and outer shells for independent leak detection of field joints, and revising the VV support system to gain a more comfortable structural performance margin. Improvements to the blanket design are also under investigation, an inter-modular key instead of two prismatic keys and a co-axial inlet-outlet cooling connection instead of two parallel pipes. One of the most important achievements in the VV R&D has been demonstration of the necessary assembly tolerances. Further development of cutting, welding and non-destructive tests (NDT) for the VV has been continued, and thermal and hydraulic tests have been performed to simulate the VV cooling conditions. In FW/blanket and divertor, full-scale prototypical mock-ups of the FW panel, the blanket shield block, and the divertor components, have been successfully fabricated. These results make us confident in the validity of our design and give us possibilities of alternate fabrication methods.

### 1. Introduction

Procurement specifications are now being prepared for ITER components whose delivery is on the critical path and required early in construction, such as the vacuum vessel. Although the basic design of the VV and in-vessel components of the ITER design has stayed the same, several detailed design improvements are being pursued in an effort to raise reliability, to improve maintainability, and to save money. R&D activities have been continued to confirm the design validity and to develop alternate cost-saving fabrication methods.

### 2. Vacuum Vessel

#### 2.1 Vacuum Vessel Design

The VV remains a double-walled torus-shaped structure of SS 316L(N)-IG, ITER Grade [1]. Design changes are being pursued to take into account fabrication methods and would provide cost benefits, such as the elimination of the inboard triangular support (see *FIG. 1*), which would simplify the VV structure and would also reduce the blanket module electromagnetic load (the poloidal torque on the inboard lowest module). The volume in the interspace between the inner and outer shells at field joint regions is now fully isolated to permit independent leak detection during VV assembly. Access for the VV thermal shield assembly, fabricability of the port stubs,

and plasma vertical stability are all helped by a design of the upper port that avoids large chamfers in connection with the main vessel. By supporting the VV at the lower ports on the cryostat floor (see *FIG. 2*), a more comfortable margin in the structural performance and better access for assembly and maintenance could be achieved. Studies of the in-vessel diagnostics design has analyzed interference with other in-vessel components. Integration of the divertor supporting structure into the VV inner shell as shown in *FIG.3*, reduces its cross-section and promises to simplify its manufacture. The rail pieces that are mechanically attached to this structure would be used for toroidal travel of the divertor cassettes during remote maintenance. A wider space is provided at the field joint area to allow access for ultrasonic testing (UT) inspection tools.

The main concept of the vacuum vessel envisages a double wall structure. However, a single wall structure is feasible in some regions (for components near to the cryostat) and is a simpler solution in VV port extensions in particular where the blanket cooling system penetrates. Most welds in the inner shell will have butt-joint configurations with both-side access and will be radiographically inspected to assure 100% weld efficiency. However, the one-sided weld joints between the outer shell and the ribs/housings, and the field joints, cannot be radiographically inspected and so will be inspected by UT or "progress LPT (liquid penetrant dye test)", and a "code case" will be justified by testing. The current approach of the weld joint configurations is to minimize required code cases.

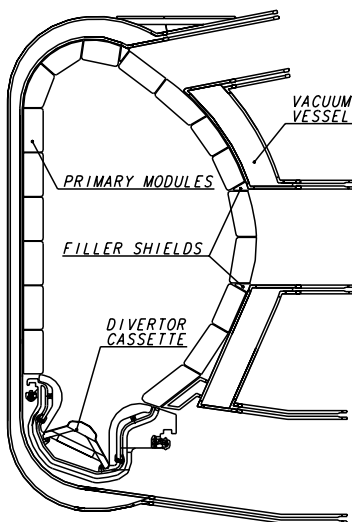


*FIG. 1* Vacuum vessel, FW/blanket and divertor

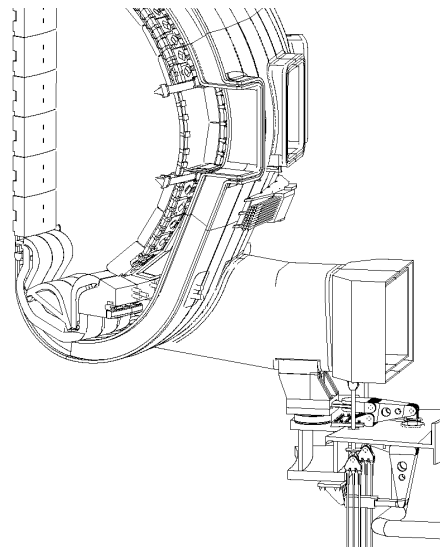


*FIG. 2* VV vertical and radial support

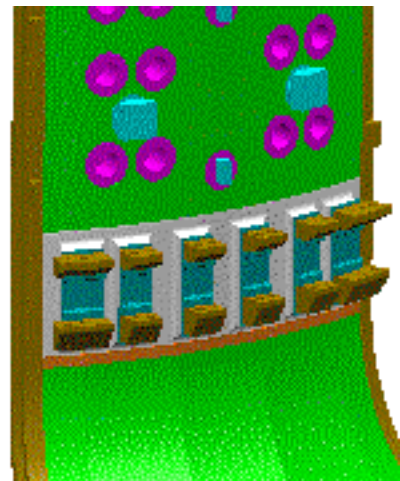


*FIG.3* Divertor support structure integrated with the VV inner shell

## 2.2 Vacuum Vessel R&D

One of the most important achievements in the VV R&D is demonstration of the necessary assembly tolerances. This has already been achieved for the main vessel, and more recently an integration test of the port extension has been performed with the full-scale sector model. As a continuous activity of VV R&D, the port extension was cut and deformation was measured to demonstrate the fabrication, assembly and maintenance[2]. A manual plasma-cutting tool was employed for this operation. Before and after the cutting work, dimensions of the VV section and

the port section were measured. Results showed no global deformation except in the port edge section, where a slight expansion up to 3-4 mm was observed. The reason can be explained by an effect of local angular distortion due to welding. During the port integration test before the port extension cutting, the remote NDT inspection of the field joint between the VV sector and the port extension was successfully performed using a robot to move a scanning device (FIG. 4). It was demonstrated that defects as small as 2-3 mm in diameter and 5mm in length can be detected for 60mm thick austenitic stainless steel plate.

Thermal-hydraulic tests have been performed to confirm the VV cooling parameters for future licensing. The tests were focused on studying (1) heat transfer in differently oriented and non-uniformly heated rectangular channels, (2) flow distribution and stability in the parallel channels at the extremely low water velocities (few mm per second), (3) development of natural circulation in the entire VV cooling circuit. The VV test element - a rectangular channel (FIG. 5) 0.2 m wide, 3 m long, 2.48 m heated length and with variable channel height (12.5, 25 or 50 mm) - has been fabricated to examine heat transfer coefficients under typical VV fluid conditions. The test conditions are pressure=1 MPa, water inlet temperature =20 and 100°C, water velocity=6.7-170 mm/s and heat flux=1.3-24.4 kW/m<sup>2</sup>. On the basis of 361 experimental results, correlations were developed describing heat transfer coefficients in the VV channels. The obtained results give confidence in the acceptable VV cooling performance, which should provide not less than 500 W/(m<sup>2</sup>K) heat transfer coefficient in the first channel at any location of the VV. Experiments with the VV two-channel model to investigate the flow distribution and its stability in the VV cooling passages are now under way. Study of the development of the natural circulation in a close to full-height (30 m) model of the entire VV cooling circuit is under preparation in order to confirm the cooling system capability of passively cooling the VV in the case of LOFI (Loss of flow incident).

As an alternative to LPT, the residue from which may compromise the vacuum purity, the novel Photothermal Camera method [3] reliably detects cracks within 0.5 mm of the surface with the inspection equipment located up to 2 metres away. A 120 W YAG laser line is raster-scanned between passes in both directions across the welded surface at a speed of 5 mm/sec and the surface temperatures concurrently recorded. By computer analysis and subtraction of the images obtained, defects are discriminated from surface irregularities and changes in reflection. In inspections carried out on weldment surfaces from narrow gap TIG in 60 mm stainless steel (shown in FIG. 6), the results proved that the Photothermal Camera is generally more sensitive and reliable than LPT and better discriminates linear (>1.6 mm) and rounded (>4 mm) flaws. The method will need to be qualified as a code case in the future. Further development of advanced methods of cutting, welding and NDT for the VV has been continued in order to increase the potential for improved cost and technical performance [3]. The main achievement of the NdYAG-Laser welding with filler wire, using up to 11 kW of power, has been to achieve stable and reliable welding of 60 mm thick SS with the following parameters: 13 passes, welding speed 0.6 m/min, deposition rate 90 g/min, deposited energy 11 kJ/cm.

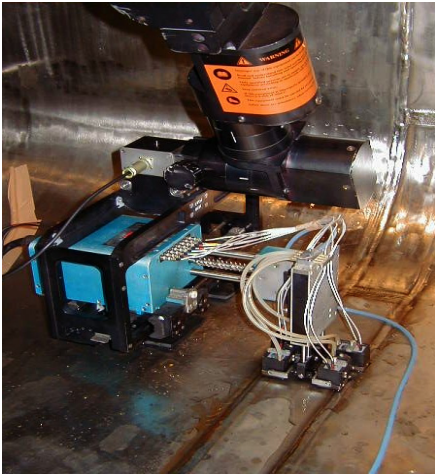


FIG. 4 UT inspection of the field joint between the VV sector and the port extension (JAPT-RFPT)

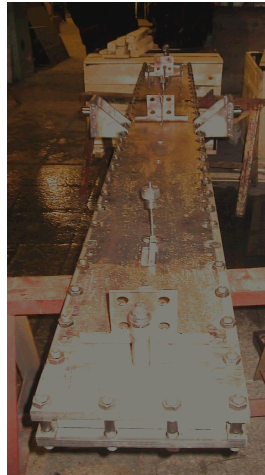


FIG. 5 VV single cooling channel model (RFPT)

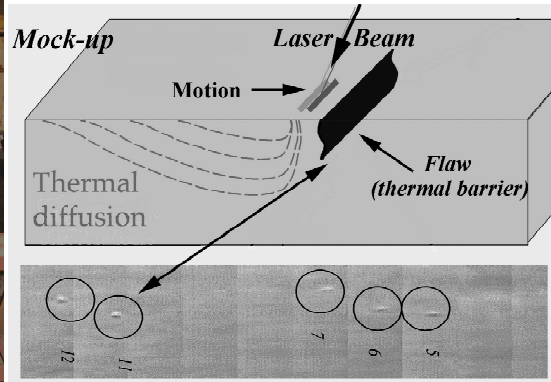


FIG. 6 Photothermal Camera as a surface crack inspection method and detected defects in a mock-up test (EUPT)

### 3. FW/Blanket

#### 3.1 FW/Blanket Design

The design of the FW/blanket system of a modular configuration, with a mechanical attachment system embedded in the vessel, is also revisited where it interfaces with the VV. As an alternative, the poloidal key design has been developed to use an inter-modular key (see FIG. 7, 8) fixed on the vessel instead of two prismatic keys. The inter-modular keys have a larger offset (1.2 m) than the prismatic keys (0.95 m) and react the radial torque ( $\sim 1$  MNm) with a lower contact force in the key. For the blanket module design with FW panels supported by a central beam, the use of a co-axial inlet-outlet cooling connection would simplify the interface with the manifolds and the VV and would facilitate the leak testing of the hydraulic connection (see FIG. 9). The design of the blanket manifolds and its end supports have been developed further to mitigate stress concentrations.

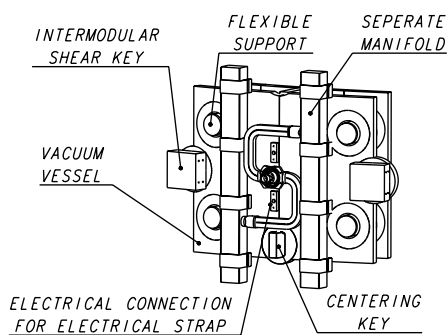


FIG. 7 Inter-modular keys, hydraulic connection and flexible supports

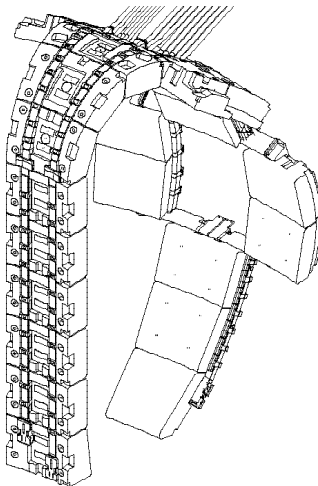


FIG. 8 Blanket modules and manifolds

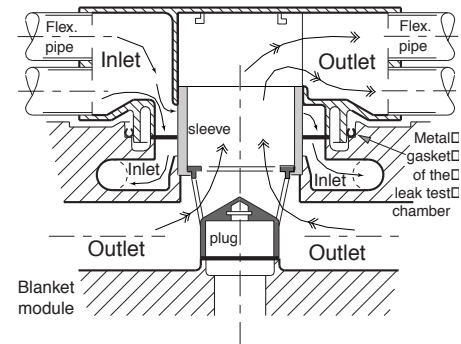


FIG. 9 Schematic view of co-axial hydraulic connector

### 3.2 FW/Blanket R&D

Blanket R&D has continued with the manufacture and testing of FW mock-ups and panel prototypes to further improve the engineering margins and to decrease the fabrication cost. It has been confirmed through recent R&D that FW mock-ups with Be tiles withstand a heat flux up to  $2.5 \text{ MW/m}^2$  for 1000 cycles or  $0.7 \text{ MW/m}^2$  for 13,000 cycles [4], which is adequate for the equivalent design requirement of  $0.5 \text{ MW/m}^2$ , 30000 cycles. Four FW panel prototypes are being fabricated to demonstrate the feasibility of HIPing (Hot Isostatic Pressing) or brazing of Be to DS-Cu or CuCrZr. Two of four FW panel prototypes have been successfully completed (see *FIG. 10*): one made from DS-Cu Al25 with Be tiles joined onto the Cu alloy by furnace brazing at  $780^\circ\text{C}$ , and the second made from CuCrZr alloy with Be tiles joined by low-temperature HIPing at  $580^\circ\text{C}$ . Both the Cu alloys were joined onto the stainless steel backing plate by solid HIPing at  $1040^\circ\text{C}$  and HIP quenching (i.e. cooling rates above  $40^\circ\text{C/min}$ ) was performed on the CuCrZr panel to keep acceptable mechanical properties of the Cu alloy. This challenging technology was applied to the full-scale FW panel prototype for the first time. Fifty-six beryllium tiles were joined onto both prototypes, and fatigue testing will be performed in the near future. The other two FW panel prototypes, one with CuAl25 and high temperature HIPed beryllium tiles, the other with powder HIPed CuCrZr and low temperature HIPed Be tiles, and one more panel with co-extruded CuCrZr/SS tubes and diffusion bonded beryllium tiles, are under construction to investigate alternative fabrication routes. The fabrication method of the Be-armoured FW was developed for the curved region at the top (or bottom) end of the FW panel by manufacturing a mock-up ( $\sim 300 \text{ mm}^{\text{W}} \times 160 \text{ mm}^{\text{H}} \times 95 \text{ mm}^{\text{L}}$ ) [5].

It is proposed to use casting to join the CuCrZr heat sink with SS and fast brazing to join Be to CuCrZr as an alternative method of the FW panel manufacturing to reduce the fabrication cost. After TIG welding of steel pipes, vacuum casting of CuCrZr was performed and followed by heat treatment: solution-annealing at  $1000^\circ\text{C}$ /water quenching/ $550^\circ\text{C}$ -6h (ultimate tensile strength is 320 MPa). Fast brazing of Be tiles was carried out in high vacuum at a temperature  $700^\circ\text{C}$ . The required heating rate ( $\sim 1.5^\circ\text{C/s}$ ) was provided by an e-beam. To check the quality of the FW mockup ( $500 \text{ mm}^{\text{L}} \times 110 \text{ mm}^{\text{W}} \times 81 \text{ mm}^{\text{H}}$ ) after casting followed by fast brazing, X-ray inspection was done (see *FIG. 11*). Thermal fatigue tests on the mockup have been successfully completed up to 5000 cycles at  $1 \text{ MW/m}^2$  followed by 500 cycles at  $1.5 \text{ MW/m}^2$ .

Fabrication of full-scale shield blocks was also completed with different cooling channel layouts: 1) a shield block with drilled poloidal cooling channels (1/2 toroidal width, i.e.  $\sim 600 \text{ mm}^{\text{W}} \times 1100 \text{ mm}^{\text{H}} \times 370 \text{ mm}^{\text{L}}$ ) and 2) a shield block with drilled radial channels (1/4 toroidal width). For the former, gouging by water jet was applied to make the deep slots. Two quarter blocks were joined by e-beam welding. The fabricated slots satisfied the specified width ( $< 10 \text{ mm}$ ) such as at the gouged region 1.5-6 mm and the EB-welded region 7.5-9.5 mm. Finally, a FW panel prototype with a central beam support was fixed onto the shield block with poloidal channels as shown in *FIG. 12* [5]. The FW panel prototype ( $\sim 300 \text{ mm}^{\text{W}} \times 1100 \text{ mm}^{\text{H}} \times 71 \text{ mm}^{\text{L}}$ ), was fabricated with satisfactory dimensional accuracy such as the slot width  $< \pm 0.5 \text{ mm}$ , the panel width  $< \pm 1 \text{ mm}$  and the step between adjacent fingers  $< 0.7 \text{ mm}$ .

Regarding the module attachment system, the Ti-alloy flexible supports and CuCrZr electrical connectors have been fabricated and tested [6]. The bolting tool used to tighten the tip of the

bolts securing the blanket module to the vessel, including preload measurement methods, has also been developed. The required preload of 800 MPa for the Inconel 718 bolts can only be achieved with an internal heater. Experiments have been carried out on using an automated water-hydraulic bolting tool with integral bolt heater. The mock-up and tooling for the co-axial hydraulic connector, which weld/cuts with new-generation CW YAG lasers, using on-line visual process control, is under construction.

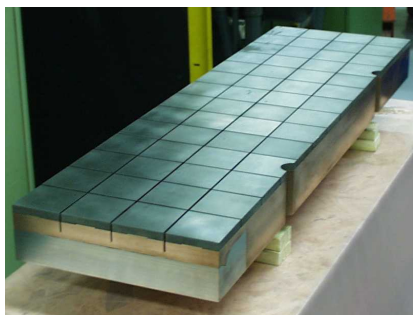


FIG. 10 One of full-scale FW panel prototypes (Be brazed to DSCu layer) (EUPT)



FIG. 11 Cast FW panel mock-up with fast brazed Be and X-ray inspection (RFPT)

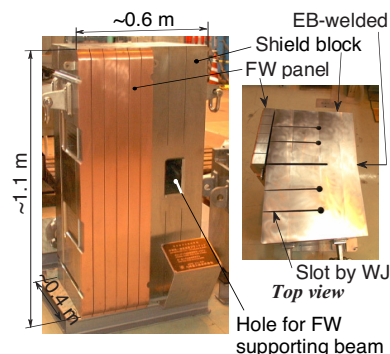


FIG. 12 Assembled FW panel prototype and shield block (1/2 toroidal width) (JAPT)

## 4 Divertor

### 4.1 Divertor Design

The ITER divertor comprises 54 cassettes onto which are mounted replaceable plasma-facing components (PFCs). The PFCs on each cassette are one inner and one outer vertical target, which intercept the plasma scrape-off layer (SOL), and a private region PFC, which restricts the flow of neutrals into the X-point and protects the gas exhaust pumping duct of the cassette from a direct view of the plasma. The region beneath the dome of the private region PFC connects the inner and outer divertor channels allowing the free flow of neutrals from inboard to outboard [7]. Carbon-fibre composite (CFC) armour is the preferred armour for the regions of the PFCs where the SOL strikes the targets and the design heat flux is  $20\text{MWm}^{-2}$ , and tungsten for all other plasma-facing surfaces of the PFCs.

### 4.2 Divertor R&D

High heat flux (HHF) testing of components with a flat tile configuration of CFC armour continue to fail at  $18\text{--}20\text{MWm}^{-2}$ , which leads to complete detachment within a few heat cycles. Hence, the CFC monoblock geometry, which has a capability up to  $\sim 30\text{MWm}^{-2}$  and has no cases recorded of tiles detaching, is maintained as the preferred option. In contrast, for the W armoured surfaces, where the heat flux  $< 5\text{MWm}^{-2}$ , both flat tile and lamellae monoblock geometries are suitable, having sustained up to 27 and  $18\text{MWm}^{-2}$  respectively.

The manufacture of CFC monoblock and W lamellae armour on the same PFC has been demonstrated on prototypical elements (see FIG. 13) with the armours joined via a cast pure Cu layer to a CuCrZr tube by low temperature HIP. HIP joining of pure Cu to CuCrZr tube at  $550^\circ\text{C}$

produces optimum mechanical properties in the CuCrZr and a grain size  $< 200\mu\text{m}$ . Ultrasonic and thermographic inspection of the prototype's joints indicates that they are of good quality and HHF testing is scheduled to begin in September 2002.

Meanwhile the feasibility has been demonstrated of using an annular flow coolant tube (see FIG. 14), which allows a more compact arrangement at the lower end of the target and the reduction of peak heat flux by elongating the target. For the hair-pin return, a hemispherical end plug radius of 7.5mm gives a pressure drop of  $0.1\text{MPa}$  at  $10\text{ms}^{-1}$ , or 17% of the total for the  $\sim 700\text{mm}$  mock-up. The design has a similar incident critical heat flux (ICHF) to that of a conventional swirl tube. A CFC-monoblock-amoured mock-up was produced using 15Cu-25Ni-60Ti braze for the CFC/OFHC Cu joint and 52Cu-10Ni-38Mn for the OFHC-Cu/CuCrZr tube joint, both brazed in the same cycle at  $980^\circ\text{C}$  for 30 min and gas quenched by Ar at  $1^\circ\text{Cs}^{-1}$  to maintain good mechanical properties in the CuCrZr. After brazing, initial cracks were observed in the CFC side wall. However, during HHF testing the mock-up survived 1000 cycles of 15s at  $20\text{MWm}^{-2}$  with no degradation of the thermal performance and no observed growth in the initial cracks.

Efforts have also focused on technologies for building PFCs using the hypervapotron cooling technique, which keeps the heat sink at  $< 500^\circ\text{C}$  during operation, avoiding over-precipitation of the CuCrZr, and hence is suitable for W flat tile armour [8]. The elements are built by casting CuCrZr onto stainless steel. A 12% reduction of the bi-metal plate obtained by rolling gives a finer grain structure and improved tensile strength. The hypervapotron ribs are formed by machining through the steel into the CuCrZr and all subsequent joints in the substrate are steel to steel. The W armour tiles are pre-coated with a cast pure Cu layer before being brazed using CuInSnNi alloy to the CuCrZr in a fast braze cycle. A 0.6m long mock-up of this design survived 1000 cycles at  $\sim 20\text{MWm}^{-2}$ .

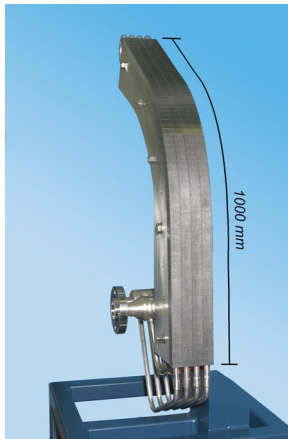


FIG. 13a Prototypical vertical target (EUPT)

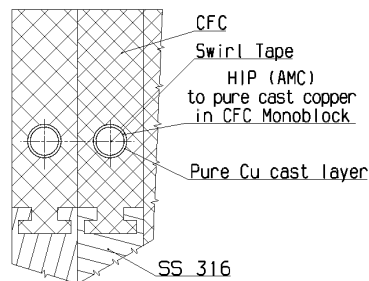


FIG. 13b Details of CFC monoblock

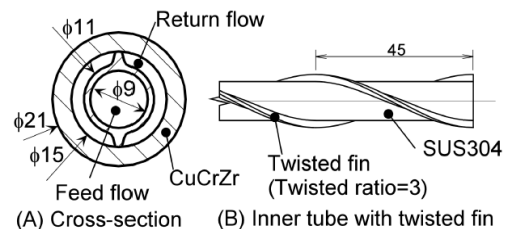


FIG. 14 Detail of annular flow coolant tube (JAPT)

The potential for the entire allowable tritium inventory of ITER to be trapped through co-deposition with sputtered carbon has long been a concern. To mitigate the problem, various design options have been proposed ranging from maintaining hot surfaces ( $\sim 800^\circ\text{C}$ ) in the private flux region to avoid local deposition, to the inclusion of a cold trap upstream of the cryopumps to prevent their contamination. The results of experiments, carried out at the Institute of Physical Chemistry, Moscow [9] and at IPP in Germany [10] suggest the following conclusions.

- 1) Due to the high ratio of atomic hydrogen to hydrocarbons, the high density in the ITER divertor and the general surface temperature  $>100^{\circ}\text{C}$ , the deposition of hydrocarbons and the survival of hydrocarbon radicals is negligible. Only stable hydrocarbon species will pass into the pumping duct and to the cryopumps where they will be processed in the normal manner. A cold trap in front of the cryopump is thus not necessary.
- 2) Surface temperatures within the private region that are greater than  $500^{\circ}\text{C}$  can promote cracking of hydrocarbons, increasing the amount of active radical species, which is not advisable. The hot radiative liner will therefore be replaced by an actively cooled component.

These laboratory experimental conclusions are very positive for the operation with CFC targets on the ITER divertor. However, experimental investigations continue both in the laboratories and the tokamaks to better understand the very complicated processes between hydrogen and carbon in the extreme conditions of a hot dense plasma and a cryogenic environment where the respective proportions  $\text{H}^0$ ,  $\text{H}_2$  and  $\text{C}_x\text{H}_y$  vary dramatically.

## 5. Conclusions

The ITER vacuum vessel and blanket design and R&D have progressed significantly in detail in collaborative efforts between the International Team and the European, Japanese, and Russian Participant Teams. The design and fabrication methods of the VV, FW/blanket and divertor have been assured by the R&D, and additional fabrication methods have also been shown to be acceptable.

## References

- [1] IOKI, K., et al., ITER-FEAT Vacuum Vessel and Blanket Design Features and Implications for the R&D Programme, Nuclear fusion Vol. 41 No. 3 (2001) 265-275.
- [2] NAKAHIRA, M., et al., Progress and achievements on the R&D activities for ITER vacuum vessel, Nuclear fusion Vol. 41 No. 4 (2001) 375-380.
- [3] JONES, L., et al., Towards advanced welding methods for the ITER vacuum vessel sectors, The 22nd Symposium on Fusion Technology, Helsinki (2002).
- [4] LORENZETTO, P., et al., ITER PFW mock-up fabrication and testing for Be/Cu alloy joining development, to be published in Fus. Eng. & Des.
- [5] KOSAKU, Y., et al., Fabrication of Prototype Mockups of ITER Shielding Blanket with Separable First Wall, JAERI-Tech 2002-063 (2002).
- [6] IOKI, K., et al., Progress on Design and R&D of ITER FW/Blanket, ISFNT-6 (2002), to be published in Fusion Engineering and Design.
- [7] KUKUSHKIN, A., PACHER, H. D.; Divertor modelling and extrapolation to reactor conditions; Plasma Phys. Control Fusion 44 (2002) 911-943.
- [8] ALIMOV, V. KH., et al., Construction and testing of divertor liner components, Task No. T436 report, IPC, Moscow, June 2001.
- [9] ARKHIPOV, I., et al., Experimental modelling of transport and deposition of methyl radicals on the cold trap of ITER-FEAT, Proc. of 15th PSI Conference, Gifu, 2001.
- [10] FUESMANN, G., et al; Construction and testing of divertor liner components; Report on Art. 5.1, Task No. T436, IPP Max-Planck-Institut fur Plasmaphysik, Berlin, June 2002.